Supporting Information

Iniesta and Shapiro 10.1073/pnas.0808807105

SI Results

The Accumulation of CpdR is Cell-Cycle Regulated. We compared the levels of CpdR and CtrA at different time points during a synchronous cell cycle by Western blot analysis, and found that CpdR accumulation peaks in late predivisional cells, following the peak of CtrA accumulation and *cpdR* transcription (Fig. S1). CpdR accumulation is minimal at the stalked cell stage, just after CtrA is cleared from the cell and DNA replication is initiated.

Note About the Half-Life of CpdR in the Presence of pP$_{xylX}$-*clpX.** In a WT strain containing the plasmid pP$_{xylX}$-*clpX**, the half-life of CpdR in the absence of xylose (Fig. 2 *A*, *solid line*) is higher than the half-life of CpdR shown in Fig. 2 *B* (*solid black line*). This difference is because of leakiness of the expression from the P$_{xylX}$ promoter, which results in some transcription of the mutated *clpX** and partial inhibition of normal ClpX function. Previous work has shown that this promoter is not tightly repressed in the absence of xylose (1).

Characterization of a DivK-Depletion Mutant Strain. We generated a DivK-depletion strain, in which an in-frame deletion of *divK* is covered by a chromosomal copy of *divK* under the control of the vanillate-inducible P$_{vanA}$ promoter (2). Upon vanillate removal, the accumulation of DivK in that mutant strain is significantly reduced after 2 h and is undetectable by Western blot analysis after 6 h (Fig. 3 *A*, *Bottom*). We compared the viability of the Δ*divK* P$_{vanA}$-*divK* strain to a strain that has both the native *divK* gene and the P$_{vanA}$-*divK* gene by spotting serial dilutions of exponential phase cultures supplemented with vanillate onto PYE plates with or without vanillate. When vanillate is removed (absence of DivK), the viability of Δ*divK* P$_{vanA}$-*divK* strain is reduced by a factor of more than 1,000 (Fig. S2 *A*, *Bottom*). In the presence of vanillate (presence of DivK), the viability is indistinguishable in both strains (see Fig. S2 *A*, *Top*). The morphology of the Δ*divK* P$_{vanA}$-*divK* cells is normal in presence of vanillate (Fig. S2 *B*, time 0) showing that the constitutive expression of *divK* does not affect cell morphology. In fact, DivK is normally present throughout the cell cycle, increasing only slightly in the late predivisional cell (3). After 4 h of vanillate removal (or DivK depletion), cells start to elongate, and after 12 h they become very filamentous (see Fig. S2 *B*).

Note About the Half-Life of CpdR$_{D51A}$ in the Absence of DivK. We have demonstrated that DivK promotes the degradation of CpdR; the half-life of CpdR in the absence of DivK was twofold longer than in its presence (see Fig. 2 *B*, *black lines*). In addition, we showed that stabilization of CpdR upon DivK depletion was dependent on the phosphorylation state of CpdR; the unphosphorylatable form of CpdR, CpdR$_{D51A,}$ was not stabilized in the absence of DivK (see Fig. 2 *B*, *gray lines*). However, the half-life of CpdR$_{D51A}$ in the absence of DivK was somewhat shorter compared to its half-life in the presence of DivK (see Fig. 2 *B*, *gray lines*). This result suggests that the presence of the DivK protein may cause a partial inhibition of CpdR degradation that is independent of the phosphorylation state of CpdR. In the absence of DivK, CpdR is maintained in its phosphorylated state and CpdR∼P cannot localize with the protease at the cell pole, resulting in an increase in its stability. Under these WT conditions, the lack of a partial inhibition of CpdR degradation, independent of its phosphorylation state, cannot be detected. However, because CpdR$_{D51A}$ does not require DivK for its localization, and therefore its degradation, in the absence of DivK, the additional inhibitory effect on CpdR degradation results in an increased degradation of CpdR$_{D51A}$. Although we do not know the mechanism of the additional effect of DivK on CpdR degradation uncovered by the use of CpdR$_{D51A}$, the main conclusion of these experiments, that DivK controls the degradation of CpdR by promoting the presence of the less stable unphosphorylated CpdR, remains valid.

CtrA Global Regulator Activates the Transcription of *cpdR*. A genome-wide analysis of CtrA-binding locations using chromatin immunoprecipitation analysis and microarrays showed that CtrA directly regulates ≈95 genes (4); included among them is *cpdR*. According to the predicted *cpdR* transcriptional start site (5), a CtrA-binding motif overlaps with the –35 position of the *cpdR* promoter sequence (Fig. S4 *A*). We fused the *cpdR* promoter to the *lacZ* gene and introduced it into the *ctrA401ts* strain, which lacks CtrA function at restrictive temperature (37°C) (6). We measured β-galactosidase activity from the strain *ctrA401ts* bearing pP$_{cpdR}$-*lacZ* at 2 and 4 h after a shift from permissive (28°C) to restrictive (37°C) temperature, and compared this to the activity at the time of the temperature shift (Fig. S4 *B*). The activity of the *cpdR* promoter was significantly decreased upon loss of CtrA function, confirming that CtrA activates *cpdR* transcription.

Effect of DivK on CpdR Phosphorylation. In an attempt to determine if DivK affects CpdR phosphorylation, we introduced a *cpdR* deletion into the DivK-depletion strain LS4400, and added a high-copy number plasmid bearing *cpdR* under the control of the xylose-inducible promoter (LS4401). This strain was grown in low phosphate media (M5G) with vanillate (presence of DivK) or without vanillate (absence of DivK). Both cultures were grown in the presence of xylose to allow constitutive *cpdR* expression, thereby eliminating the transcriptional effect of CtrA on *cpdR* expression (see Fig. S4 *B*). After 12 h, an aliquot of each culture was labeled for 5 min with [γ-^{32}P]-ATP. Immunoprecipitation and Western blot analyses using anti-CpdR antibodies were performed to compare the amount of CpdR∼^{32}P phosphorylated during the labeling period and the level of total CpdR protein (Fig. S3). In the absence of DivK, the amount of both CpdR∼^{32}P and total CpdR protein were higher than in the presence of DivK.

SI Materials and Methods

Construction of Plasmids. Plasmids used in this study are presented in Table S1. Primer sequences that are not complementary to the template are indicated in boldface.

Plasmid pP$_{cpdR}$-*lacZ*. The *cpdR* promoter region (577 bp upstream and 39 bp downstream from the translational start site) was amplified by PCR using the primers Orf03749.frontORR7 (5′-**CCCAAGCTT**GACGCGGGGAATCGTACCCA-3′) and 0744_F1R1 (5′-**GGAATTC**GCGCAGGGAATCATCGTCTTC-3′) and *Caulobacter* NA1000 genomic DNA as a template. The product was cloned into pCR-Blunt II-TOPO (Invitrogen) generating plasmid pTOPO-P$_{cpdR}$. A PstI/SpeI-fragment from pTOPO-P$_{cpdR}$ containing the whole *cpdR* promoter region was cloned into PstI/XbaI-digested p*lacZ290* vector (J.W. Gober and M.R. Alley, unpublished), for *lacZ* transcriptional fusion.

Plasmid pP_{vanA}-*divK*. The *divK* coding region was amplified by PCR using the primers DivK.for (5′-CGCCACGTGACC**AT**ATGGTCGGGGTAAGG-3′) and DivK.rev (5′-**GGAATTC**CCGGGCGCTCATGCAGGCTGCCTTTC-3′) and *Caulobacter* NA1000 genomic DNA as a template. The PCR product was cut with NdeI and EcoRI, and cloned into NdeI/EcoRI-digested into pVCHYN-4 (2) for the integration of *divK* at the chromosomal *vanA* locus.

Plasmid pP_{xylX}-*cpdR*/pP_{xylX}-$cpdR_{D51A}$. The whole *cpdR*/$cpdR_{D51A}$ coding region was amplified by PCR using the primers RR7Xyl.for (5′-GGACACGTGACC**AT**ATGGCCCGCATCC-3′) and RR7Xyl.rev (5′-**CGGGATCC**CGGATCAGGCCGCCAT-CATC-3′) and NA1000 genomic DNA/p$cpdR_{D51A}$ plasmid (7) as a template. The PCR product was digested by NdeI and BamHI and cloned into equally treated pXGFP4-C1 vector (M.R. Alley, unpublished), which contains the *xylX* promoter, generating plasmid pAA227/pAA228. Using pAA227/pAA228 as a DNA template and the primers Pxyl500.for (5′-**GGGAATTC**CAC-CAGCCACAGGCCCGTGC-3′) and RR7Xyl.rev, *cpdR*/$cpdR_{D51A}$ coding region fused to 500 bp of the *xylX* promoter region was amplified by PCR. The product was digested by EcoRI and BamHI and cloned into equally treated pM31 expression vector (high-copy number plasmid, Cm^R) (R. Roberts, unpublished), generating plasmid pP_{xylX}-*cpdR*/pP_{xylX}-$cpdR_{D51A}$.

Construction of Strains. The strains used in this study are presented in Table S2.

Strain **LS4398** was generated by introducing plasmid pP_{cpdR}-*lacZ* into strain *ctrA401ts* (6).

Strain **LS4399** was generated by integration of plasmid pP_{vanA}-*divK* at the *vanA* locus of strain NA1000 by single homologous recombination.

Strain **LS4400**: plasmid pEΔ*divK*H-NPTS138 was integrated at the *divK* locus of strain LS4399 by single homologous recombination, obtaining strain LS4412. Plasmid pEΔ*divK*H-NPTS138 (D. Hung, unpublished), a $K_m{}^R$ pNPTS138-based plasmid (Litmus 38-derived vector with *oriT*, *sacB* and *npt1* genes) (M.R. Alley, unpublished), is an integration plasmid for the generation of a chromosomal deletion of *divK* (45 to 350 bp after translational start site). Strain LS4412 was grown to stationary phase in PYE medium with 0.5-mM vanillate lacking kanamycin. The cells were subsequently spread on PYE plates containing 0.5-mM vanillate and 3% sucrose and incubated at 28°C. Single colonies were picked and transferred in parallel onto plain PYE plates and PYE plates containing kanamycin. Kanamycin-sensitive clones, which had lost the integrated plasmid because of a second recombination event, were confirmed for the presence of the *divK* deletion allele by colony PCR.

Strain **LS4401**: The in-frame Δ*cpdR* deletion was introduced into strain LS4400 by transduction with a ΦCr30 lysate of strain LS4177 (7), resulting in strain LS4413. Plasmid pP_{xylX}-*cpdR* was introduced into LS4413.

Strain **LS4402** was generated by introducing plasmid pP_{xylX}-$cpdR_{D51A}$ into strain LS4413.

Strain **LS4403** was generated by introducing plasmid pP_{xylX}-*cpdR-yfp* into strain LS4413.

Strain **LS4404** was generated by introducing plasmid pP_{xylX}-$cpdR_{D51A}$-*yfp* into strain LS4413.

Strain **LS4405**: *clpX-gfp* was inserted into the *xylX* locus of strain LS4400 by transduction with ΦCr30 lysate of strain LS4183 (8), obtaining strain LS4414. Plasmid pP_{xylX}-*cpdR* was introduced into strain LS4414.

Strain **LS4406**: The plasmid pΔ*fixT* (pNPTS138-based plasmid) (9) was integrated into the *fixT* locus of the strain LS4218 (containing chromosomal $cpdR_{D51A}$) (7). *fixT* (CC0753) and *cpdR* (CC0744) are genetically linked; therefore, we simultaneously introduced pΔ*fixT* and $cpdR_{D51A}$ into strain LS4400 by generalized transduction, obtaining strain LS4415. The presence of $cpdR_{D51A}$ was confirmed by sequencing. Strain LS4415 was grown to stationary phase in PYE medium lacking kanamycin. The cells were subsequently spread on PYE plane plates. Single colonies were picked and transferred in parallel onto plain PYE plates and PYE plates containing kanamycin. Kanamycin-sensitive clones, which had lost the integrated plasmid because of a second recombination event, were confirmed for the presence of the *fixT* allele by colony PCR, resulting in strain LS4416. *clpX-gfp* was inserted into the *xylX* locus of strain LS4416 by transduction with ΦCr30 lysate of strain LS4183 (8), obtaining strain LS4417. Finally, plasmid pP_{xylX}-$cpdR_{D51A}$ was introduced into strain LS4417.

Strain **LS4407**: Plasmid pP_{xylX}-*yfp-ctrA-RD-15* was introduced into strain LS4400, generating the strain LS4418. Plasmid pP_{xylX}-*cpdR* was introduced into strain LS4418.

Strain **LS4408**: Plasmid pP_{xylX}-*yfp-ctrA-RD-15* was introduced into strain LS4419, generating the strain LS4420. Plasmid pP_{xylX}-$cpdR_{D51A}$ was introduced into strain LS4420.

Strain **LS4409** was generated by introducing plasmid pP_{xylX}-*cpdR* into strain LS4177 (Δ*cpdR*) (7).

Strain **LS4410** was generated by introducing plasmid pP_{xylX}-$cpdR_{D51A}$ into strain LS4177 (Δ*cpdR*) (7).

Strain **LS4411** was created by introducing plasmid pP_{xylX}-*cplX** (pMO88) (10) into strain NA1000.

Generalized transduction was performed with the phage ΦCr30 following a previously described procedure (11).

Electroporation of *Caulobacter crescentus*. Electroporation conditions were modified from the protocol used for *Myxococcus xanthus* (12). Stationary-phase *Caulobacter* cultures (3–5 ml) were pelleted by centrifugation at 16,000 × *g*, 25°C, for 1 to 2 min. The cell pellet was suspended in one volume of sterile water and centrifuged, repeating the process three times. The cell pellet was then suspended in 80 to 150 μl of water, mixed with plasmid DNA (1 μl for replicating plasmids [0.1–1 μg], or 12 μl for integrating plasmids [1.2–12 μg]), transferred to a 1- to 2-mm electrode gap cuvette, and electroporated at 1.5 kV, 400 Ω, and 25 μF. Cells were flushed from the cuvette with 2 ml of PYE media and incubated at 28°C for 3 to 4 h. After this recovery period, cells were plated on PYE plates with the appropriate antibiotic.

***cpdR* Promoter Activity Assays.** The β-galactosidase activity of P_{cpdR}-*lacZ* was assayed in log-phase cultures and determined according to Miller (13). β-gal activities represent the average of four independent assays, and the standard error of the mean was calculated.

***In Vivo* Phosphorylation Assays.** *In vivo* phosphorylation experiments were performed as previously described (14), using 30 μCi of Easytides Adenosine 5′-Triphosphate [gamma-^{32}P] (PerkinElmer) per 1 ml of culture for 5 min. Each sample was immunoprecipitated with 10 μl of anti-CpdR antibody.

Immunoblot Analysis. The isolation of swarmer cells was performed using Ludox AS-40 (Sigma-Aldrich) as described previously (11). Cells were pelleted, resuspended in SDS sample buffer, and boiled for 4 min. The proteins were then separated on 12 to 15% SDS-polyacrylamide gels and transferred to a PVDF membrane (Immobilon, Millipore). Immunodetection was performed with rabbit antisera directed against CpdR (7), CtrA (14), or DivK (3) at dilutions of 1:500 (CpdR), or 1:10,000 (CtrA), or 1:5,000 (DivK), respectively, using standard procedures. Donkey anti-rabbit immunogloblulin G conjugated to HRP (Jackson ImmunoResearch) was used as secondary antibody. Immunocomplexes were visualized using the Western

Lightning chemiluminescence reagent (PerkinElmer) and Kodak Bio-Max MR film. Images were processed with Photoshop (Adobe), and relative band intensities were determined using ImageQuant software (Molecular Dynamics).

Pulse-Chase Experiments. Cells were grown in M2G media to an $O.D._{660}$ of 0.3 and pulsed with 10-μCi/ml Redivue L-[^{35}S]-methionine (Amersham) for 2 min. To chase, 1-mM unlabeled L-methionine and 0.2-mg/ml casamino acids were added to the culture. One ml of culture was collected every 10 or 20 min after chase, pelleted by centrifugation, and frozen on dry ice. The cell pellet was resuspended in 50 μl of SDS buffer (10-mM Tris-HCl pH 8, 1% SDS, 1-mM EDTA) and boiled for 4 min to lyse the cells. Cell lysate was then mixed with 800 μl of immunoprecipitation (IP) wash buffer (50-mM Tris-HCl pH 8, 150-mM NaCl, 0.5% Triton X-100) and 20 μl of protein A-agarose (Roche) and incubated for 1 h at room temperature to precipitate proteins that bind nonspecifically. Equivalent counts of radiolabelled proteins (generally 700 μl of the precleared supernatant) were used for immunoprecipitation. Each sample was rocked gently with 10 μl of anti-CpdR serum (7) at room temperature for 1 h and then with 20 μl of protein A-agarose at room temperature for 1 h. The immunoprecipitate was collected by centrifugation, washed three times with IP wash buffer, resuspended in 25 μl of SDS sample buffer, and boiled for 4 min. The resulting samples were resolved by 15% SDS-polyacrylamide gels. The gel was dried and exposed against a Phosphor Screen (Molecular Dynamics) for at least 20 h. Labeled protein bands were scanned and quantified using a PhosphorImager with ImageQuant software (Molecular Dynamics). Line fitting and error calculation was performed using KaleidaGraph 4.0 with all unaveraged time points from two to three independent experiments. For clarity of presentation, the data points presented in the graph represent the average at each different time point.

1. Meisenzahl AC, Shapiro L, Jenal U (1997) Isolation and characterization of a xylose-dependent promoter from *Caulobacter crescentus. J Bacteriol* 179:592–600.
2. Thanbichler M, Iniesta AA, Shapiro L (2007) A comprehensive set of plasmids for vanillate- and xylose-inducible gene expression in *Caulobacter crescentus. Nucleic Acids Res* 35:e137.
3. Jacobs C, Hung D, Shapiro L (2001) Dynamic localization of a cytoplasmic signal transduction response regulator controls morphogenesis during the *Caulobacter* cell cycle. *Proc Natl Acad Sci USA* 98:4095–4100.
4. Laub MT, Chen SL, Shapiro L, McAdams HH (2002) Genes directly controlled by CtrA, a master regulator of the *Caulobacter* cell cycle. *Proc Natl Acad Sci USA* 99:4632–4637.
5. McGrath PT, *et al.* (2007) High-throughput identification of transcription start sites, conserved promoter motifs and predicted regulons. *Nat Biotechnol* 25:584–592.
6. Quon KC, Marczynski GT, Shapiro L (1996) Cell cycle control by an essential bacterial two-component signal transduction protein. *Cell* 84:83–93.
7. Iniesta AA, McGrath PT, Reisenauer A, McAdams HH, Shapiro L (2006) A phospho-signaling pathway controls the localization and activity of a protease complex critical for bacterial cell cycle progression. *Proc Natl Acad Sci USA* 103:10935–10940.
8. McGrath PT, Iniesta AA, Ryan KR, Shapiro L, McAdams HH (2006) A dynamically localized protease complex and a polar specificity factor control a cell cycle master regulator. *Cell* 124:535–547.
9. Crosson S, McGrath PT, Stephens C, McAdams HH, Shapiro L (2005) Conserved modular design of an oxygen sensory/signaling network with species-specific output. *Proc Natl Acad Sci USA* 102:8018–8023.
10. Potocka I, Thein M, ØSterås M, Jenal U, Alley MR (2002) Degradation of a Caulobacter soluble cytoplasmic chemoreceptor is ClpX dependent. *J Bacteriol* 184:6635–6641.
11. Ely B (1991) Genetics of *Caulobacter crescentus. Methods Enzymol* 204:372–384.
12. Kashefi K, Hartzell PL (1995) Genetic suppression and phenotypic masking of a *Myxococcus xanthus frzF*-defect. *Mol Microbiol* 15:483–494.
13. Miller JH (1972) *Experiments in molecular genetics.* (Cold Spring Harbor Laboratory Press, Cold Spring Harbor, New York).
14. Domian IJ, Quon KC, Shapiro L (1997) Cell type-specific phosphorylation and proteolysis of a transcriptional regulator controls the G1-to-S transition in a bacterial cell cycle. *Cell* 90:415–424.
15. Ryan KR, Judd EM, Shapiro L (2002) The CtrA response regulator essential for *Caulobacter crescentus* cell-cycle progression requires a bipartite degradation signal for temporally controlled proteolysis. *J Mol Biol* 324:443–455.
16. Evinger M, Agabian N (1977) Envelope-associated nucleoid from *Caulobacter crescentus* stalked and swarmer cells. *J Bacteriol* 132:294–301.

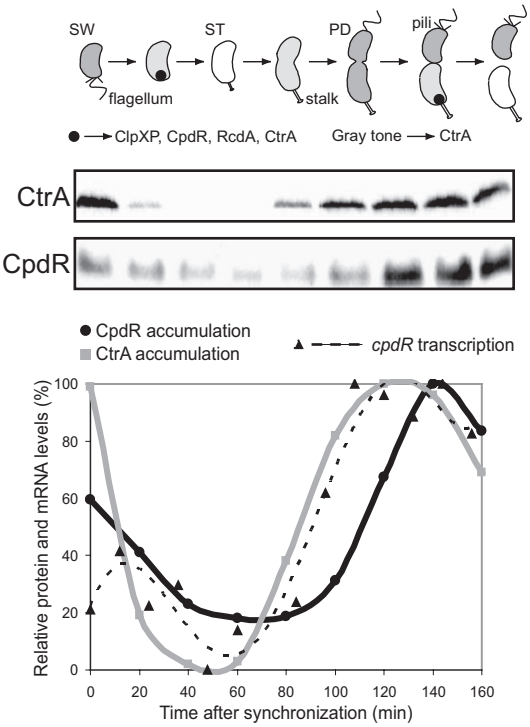

Fig. S1. A schematic of the *Caulobacter* cell cycle showing the cell cycle accumulation of CtrA (*gray tone*) and the transient polar localization of the ClpXP-CpdR-RcdA-CtrA complex (*Upper*). The accumulation of CtrA and CpdR was detected by Western blot analysis using anti-CtrA and anti-CpdR antibodies at different time points during growth of synchronized cultures (*Middle*). The relative amounts of CtrA (*gray line*) and CpdR (*solid black line*) and *cpdR* mRNA levels (*dashed line and triangles*) vary during the cell cycle (*Bottom*). *cpdR* mRNA levels were derived from microarray experiments using an Affymetrix *Caulobacter* whole genome array (5). PD, predivisional cell; ST, stalked cell; SW, swarmer cell.

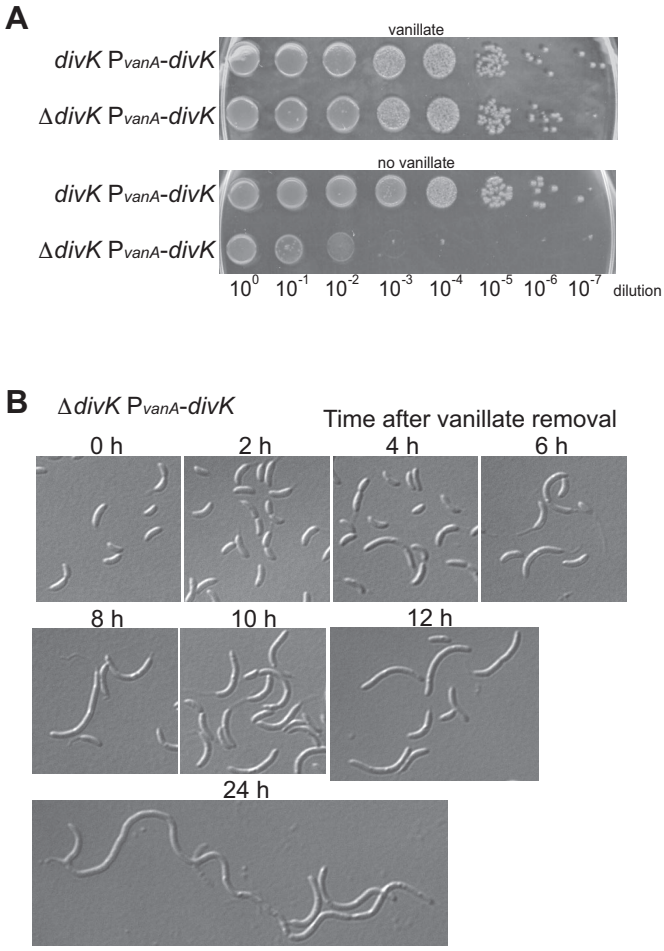

Fig. S2. Characterization of the DivK depletion mutant strain. (*A*) Viability assays on PYE plates. Cells from the strains P_{vanA}-*divK* (with a WT *divK* at its own locus) and Δ*divK* P_{vanA}-*divK* were grown to exponential phase in PYE media containing vanillate (0.5 mM). The cultures were serially diluted; 5 μl of each diluted sample was spotted on PYE plates with or without vanillate. In the presence of vanillate, the viability of both strains is similar (*Upper*); but in the absence of vanillate, the viability of the cells bearing only one copy of *divK* at the vanillate-inducible promoter decreased more than a 1,000-fold (*Bottom*). (*B*) Morphology of the Δ*divK* P_{vanA}-*divK* cells after DivK depletion by vanillate removal. Cells were grown in M2G media under exponential growth conditions in the presence of vanillate, then vanillate was removed and images of the cells were taken at the indicated times. Cell morphology is normal in the presence of DivK (0 h), and cell elongation occurs after 6 h, with significant filamentation after 12 h.

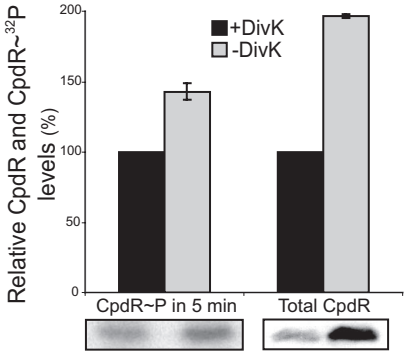

Fig. S3. Amount of CpdR~P that is phosphorylated in 5 min and total CpdR protein levels from Δ*cpdR* Δ*divK* P_{vanA}-*divK* pP_{xylX}-*cpdR* cells grown in M5G medium in the presence or absence of vanillate (after 12 h of DivK depletion). Results from three independent assays were averaged and the standard error of the mean calculated.

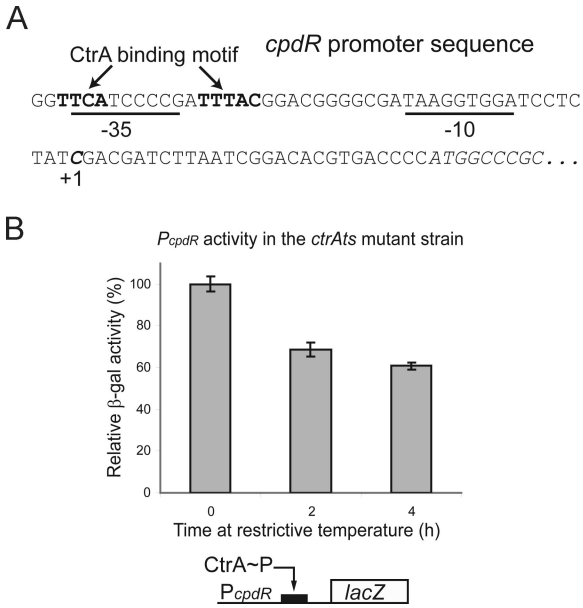

Fig. S4. CtrA activates the *cpdR* promoter. (*A*) Schematic of the *cpdR* promoter sequence showing the CtrA-binding motif, the predicted transcriptional start site (5), and the predicted –35 and –10 positions. (*B*) *Caulobacter ctrA401ts* mutant strain containing the plasmid pP_{cpdR}-*lacZ* was grown in PYE media at permissive temperature (28°C) under exponential growth conditions. After a shift to the restrictive temperature (37°C), β-galactosidase activity was measured in culture samples taken at the indicated times. The black box in the schematic represents a CtrA-binding site in the *cpdR* promoter.

Table S1. Relevant plasmids

Plasmid	Relevant genotype/description	Reference
pP_{cpdR}-*lacZ*	*cpdR* promoter fused to the *lacZ* gene, Tet^R	This study
pP_{vanA}-*divK*	*divK* under P_{vanA} promoter, Gm^R	This study
pP_{xylX}-*cpdR*	*cpdR* under P_{xylX} promoter, Cm^R	This study
pP_{xylX}-$cpdR_{D51A}$	$cpdR_{D51A}$ under P_{xylX} promoter, Cm^R	This study
pP_{xylX}-*cpdR-yfp*	*cpdR* 3′ fused to *eyfp* under P_{xylX} promoter, Cm^R	(7)
pP_{xylX}-$cpdR_{D51A}$-*yfp*	$cpdR_{D51A}$ 3′ fused to *eyfp* under P_{xylX} promoter, Cm^R	(7)
pP_{xylX}-*yfp-ctrA*$_{RD}$-15	Plasmid pEJ146, Km_R	(15)
pP_{xylX}-*cpIX**	Plasmid pMO88, Tet^R	(10)

Table S2. Relevant strains

Strain	Relevant genotype/description	Reference
CB15N	Synchronizable derivate of wild-type strain CB15 (NA1000)	(16)
LS2195	*ctrA401ts*	(6)
LS4398	*ctrA401ts* pP_{cpdR}-*lacZ*	This study
LS4399	P_{vanA}-*divK*	This study
LS4400	Δ*divK* P_{vanA}-*divK*	This study
LS4401	Δ*cpdR* Δ*divK* P_{vanA}-*divK* pP_{xylX}-*cpdR*	This study
LS4402	Δ*cpdR* Δ*divK* P_{vanA}-*divK* pP_{xylX}-$cpdR_{D51A}$	This study
LS4403	Δ*cpdR* Δ*divK* P_{vanA}-*divK* pP_{xylX}-*cpdR-yfp*	This study
LS4404	Δ*cpdR* Δ*divK* P_{vanA}-*divK* pP_{xylX}-$cpdR_{D51A}$-*yfp*	This study
LS4405	Δ*divK* P_{vanA}-*divK* P_{xylX}-*clpX-gfp* pP_{xylX}-*cpdR*	This study
LS4406	Δ*divK* P_{vanA}-*divK* P_{xylX}-*clpX-gfp cpdR*::$cpdR_{D51A}$ pP_{xylX}-$cpdR_{D51A}$	This study
LS4407	Δ*divK* P_{vanA}-*divK* pP_{xylX}-*yfp-ctrA*-$_{RD}$-$_{15}$ pP_{xylX}-*cpdR*	This study
LS4408	Δ*divK* P_{vanA}-*divK cpdR*::$cpdR_{D51A}$ pP_{xylX}-*yfp-ctrA*-$_{RD}$-$_{15}$ pP_{xylX}-$cpdR_{D51A}$	This study
LS4409	Δ*cpdR* pP_{xylX}-*cpdR*	This study
LS4410	Δ*cpdR* pP_{xylX}-$cpdR_{D51A}$	This study
LS4411	NA1000 pP_{xylX}-*cplX**	This study